

Article

Thermoeconomic Evaluation of Modular Organic Rankine Cycles for Waste Heat Recovery over a Broad Range of Heat Source Temperatures and Capacities

Markus Preißinger * and Dieter Brüggemann

Lehrstuhl für Technische Thermodynamik und Transportprozesse, Zentrum für Energietechnik, Universität Bayreuth, Universitätsstraße 30, 95447 Bayreuth, Germany; lttt@uni-bayreuth.de or zet@uni-bayreuth.de

* Correspondence: markus.preissinger@uni-bayreuth.de; Tel.: +49-921-55-7285

Academic Editor: Andrew J. Haslam

Received: 2 January 2017; Accepted: 21 February 2017; Published: 24 February 2017

Abstract: Industrial waste heat recovery by means of an Organic Rankine Cycle (ORC) can contribute to the reduction of CO₂ emissions from industries. Before market penetration, high efficiency modular concepts have to be developed to achieve appropriate economic value for industrial decision makers. This paper aims to investigate modularly designed ORC systems from a thermoeconomic point of view. The main goal is a recommendation for a suitable chemical class of working fluids, preferable ORC design and a range of heat source temperatures and thermal capacities in which modular ORCs can be economically feasible. For this purpose, a thermoeconomic model has been developed which is based on size and complexity parameters of the ORC components. Special emphasis has been laid on the turbine model. The paper reveals that alkylbenzenes lead to higher exergetic efficiencies compared to alkanes and siloxanes. However, based on the thermoeconomic model, the payback periods of the chemical classes are almost identical. With the ORC design, the developed model and the boundary conditions of this study, hexamethyldisiloxane is a suitable working fluid and leads to a payback period of less than 5 years for a heat source temperature of 400 to 600 °C and a mass flow rate of the gaseous waste heat stream of more than 4 kg/s.

Keywords: Organic Rankine Cycle; thermoeconomics; waste heat recovery; modular design; siloxane; cost function

1. Introduction

The Organic Rankine Cycle (ORC), a thermodynamic cycle which is based on organic working fluids instead of water, has been widely discussed to exploit a broad range of renewable heat sources. However, only for geothermal heat sources and in biomass fired power plants, business cases for economic feasibility have been found and market penetration has been reached in the last decades. For geothermal heat sources, the drilling costs are predominant compared to the cost of the ORC. Therefore, tailor-made power plants with partly cost intensive methods to increase the efficiency, e.g., double-stage design, are still profitable. For biomass, profitability is increased by selling standardized units including thermal oil circuit to connect ORC and biomass combustion to a wide range of customers (economy of volume).

Furthermore, ORC has attracted interest for industrial decision makers in terms of waste heat recovery as the member states of the European Union have committed themselves to increase energy efficiency by 20% by 2020 [1]. Increasing the energy efficiency in industry plays a key role to reach this goal. In many processes, large amounts of hot air or flue gasses are disposed of a chimney being potential ORC heat sources. However, typical payback periods must be achieved even without

politically imposed subsidies but with market level electricity costs. This is only possible if highly efficient ORC units with low specific investment costs are designed. Hence, it is necessary to identify efficient working fluids and ORC designs including the advantages of economy of volume.

Concerning fluid selection, thermodynamic process simulations are mostly carried out for some countable number of ORC working fluids available in some kind of simulation program (see e.g., highly cited publications and review papers [2–5]). A review of more advanced methods based on the powerful Computer Aided Molecular Design (CAMD) tool is given by Linke et al. [6]. Schwoebel et al. [7,8] screened more than 72 million chemical substances from the public available PubChem database. Regardless of the applied methodology, one major drawback of almost all available publications is the focus on a specific temperature level of the heat source. However, investigation of a broad range of heat source temperatures is necessary to design a modular ORC for waste heat recovery which can be applied in several different applications [9]. Furthermore, the influence of ORC scale is mostly neglected in the literature. However, this is a crucial aspect of waste heat recovery in industries. If ORC units are too small, specific investment costs increase dramatically due to economy of scale (in the chemical industry, the 6/10th-factor is often applied as a rule of thumb in this context [10,11]). However, the smaller ORC units represent a higher possible number of sold units (economy of volume). Lastly, literature lacks on appropriate data on the dependence between increased complexity of ORC design and increasing specific costs [12].

Hence, Colonna et al. [13] identified in their overview on ORC technology a gap in the current literature for thermoeconomic investigation of modular-based ORC units for industrial waste heat recovery. This paper aims to contribute to this field of research by proving the following hypothesis:

“It is possible to develop a thermoeconomic model for modular-based ORC units which helps to identify suitable working fluids and plant configurations that lead to economically feasible waste heat recovery plants in industry for a broad range of heat source temperatures and thermal capacities.”

The hypothesis can be broken down to the following research questions answered in this study:

1. Which chemical class of ORC working fluids can be applied in a wide range of heat source temperatures?
2. Which ORC design is favorable to cover also a broad range of heat source thermal capacities?
3. Which aspects must be included in a thermoeconomic model to allow for a robust and holistic evaluation of modular ORC units?
4. For which range of heat source temperatures and thermal capacities are ORC units economically feasible?

2. Theory

2.1. Industrial Waste Heat

Data on the amount of industrial waste heat are scarce for most of the countries and regions worldwide. Some studies give the potential of the electric power in GW which can be generated in an ORC, other focus on the thermal energy generally given in TWh. Figure 1 gives an overview of available data where each point in the diagram represents data from one of the following studies. The energy supplier Enova SF from Sweden carried out a study with a bottom-up approach by surveying 72 industrial sites [14]. Based on annual operating hours of 8760 h, 0.8 GW electric power can be obtained from waste heat above 140 °C. Pehnt et al. [15] adapted the study to Germany and published a value of 10.0 GW. A further study for Germany gives a potential of 2.5 GW in the temperature range from 80 °C to 300 °C [16]. Hamm et al. [17] specified a potential of 0.6 GW for Germany, 2.4 GW for the EU15 and 22.4 GW worldwide. Further studies include the Austrian cement industry with 6.8 MW [18], the United States with 750 MW [19] and the Canadian energy

intensive industry with 8.1 GW [20]. The potential for Canada is consistent with the value given by Zhang [21] (10.9 GW), however, the two values for the US (750 MW compared to 35 GW) differ significantly. The U.S. Department of Energy [22] determined a potential of 3.02 GW for temperatures lower than 230 °C, 2.34 GW for 230 °C to 650 °C and 0.72 GW for temperatures higher than 650 °C. For the UK, four different values (171 MW, 309 MW, 338 MW and 685 MW) are given [23]. Lastly, Campana et al. [24] calculated a potential of 2.7 GW for EU27. To summarize, it can be stated that for industrial waste heat:

- The values for the electric power potential from waste heat recovery differ significantly, however, it is a common fact that a huge potential is available.
- The thermal capacity of industrial waste heat flows strongly depends on application ranging from a few kW up to several MW.
- Industrial waste heat covers a broad range of heat source temperature, however, 300 °C and 600 °C seems to be a promising range for electricity generation from waste heat [25].

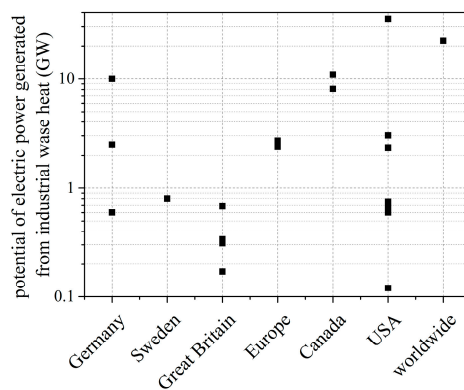


Figure 1. Potential of electric power generated from industrial waste heat in different regions (operating hours: 8760 h/a).

It is obvious from these results that the approach of modular ORC units which can serve a broad range of heat source temperature and thermal capacity is highly relevant for market penetration of ORC in the field of industrial waste heat recovery.

2.2. Organic Rankine Cycle

The basic ORC in Figure 2 (left) consists of just four components: pump, heater, expander, and condenser. The pump can be a continuous-flow or a displacement machine. The low viscosity of most organic fluids leads to reciprocating pumps, like for example piston diaphragm pumps, especially for mini- and small-scale applications. For medium- and large-scale geothermal plants, centrifugal pumps are common. Depending on heat transfer rate, temperature and pressure, shell and tube heat exchangers, plate heat exchangers or plate-and-shell heat exchangers are applied in state-of-the-art ORC units. For high absolute temperature and temperature change as well as for high pressure, mostly shell-and-tube heat exchangers are chosen. In biomass fired power plants and high-temperature waste heat recovery from industries, an additional thermal oil circuit is still used to protect the working fluid from thermal degradation [3,26–28]. Different types of expander have been discussed in literature and are applied in commercial ORC units. In mini- and small-scale applications, scroll expanders are often used. The volume flow ratio between outlet and inlet is in the range of 2.7 to 5.4, isentropic efficiency ranges from 42% to 68% [29–31]. Screw expanders are an alternative to scroll expanders especially for wet working fluids (negative slope of the dew line) as gap losses are reduced for vapor fractions of 80% to 95% [32,33]. Next to volumetric expanders, turbomachines are commonly applied in medium-

to large-scale and frequently discussed for small-scale applications. Brasz et al. [34,35] investigated radial turbines, while Klonowicz et al. [36,37] studied hermetically sealed turbo-generator-units.

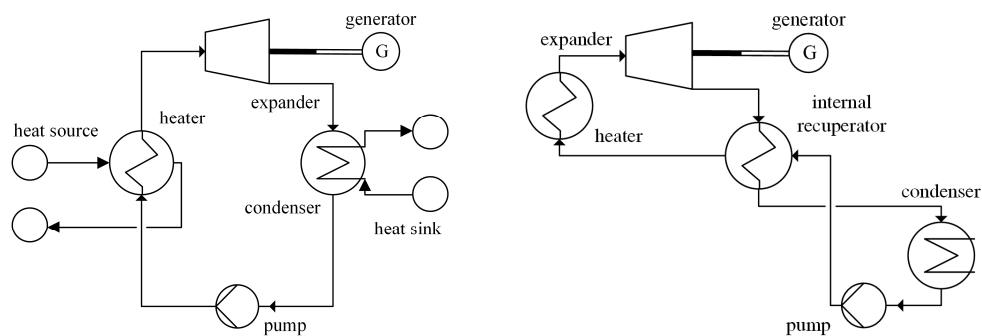


Figure 2. Scheme of Organic Rankine Cycle plant (**left:** basic ORC with heat source and heat sink; **right:** ORC including internal recuperator (heat source and sink aren't shown for clarity reasons)).

To increase the efficiency of ORC units compared to the basic configuration, approaches with and without additional components have to be distinguished. For the latter, the most commonly known are the integration of an internal recuperator [38–41], additional preheating of the working fluid by use of an economizer [42,43] and multi-stage processes [44–52]. Methods without additional components mainly focus on improving the temperature match between heat source, working fluid and environment. In this context, fluid mixtures lead to temperature glide during evaporation and condensation [53–55]. For supercritical mode of operation, phase change just occurs in the condenser but not in the heater. Compared to the basic ORC, efficiency increase can only be achieved by the better temperature match in the heater [56–60].

3. Methodology

3.1. Approach for Modular Design of ORC Units

Due to the variability of heat source characteristics in industrial processes, ORC units have to be adjusted on a case by case based on the heat source temperature and mass flow rate. This tailor-made approach is both time- and cost-intensive. From an engineering point of view, modularly-designed ORC units could be a solution to reduce the costs. In the best case, it would be possible to use one and the same concept for a broad range of temperature and power by slightly adjusting only one reference plant (see Figure 3). To develop such a module and apply it in industrial waste heat recovery, the ORC configuration has to be simple and robust but highly efficient at the same time.

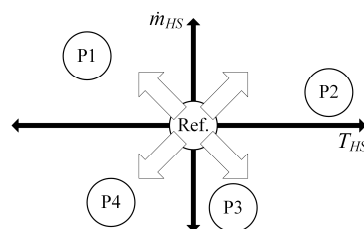


Figure 3. Approach of modular design: derive different plants P1 to P4 for various heat source temperatures and mass flow rates from one reference plant (Ref.).

Based on the literature described in the previous section, a single-stage ORC with internal recuperator in sub- and supercritical mode of operation is chosen for subsequent analysis. Pure fluids are used, as fluid mixtures lead to a significant increase in heat exchange area [61]. The IR increases the thermal efficiency for dry working fluids and reduces the cooling of the heat source so that acid

formation is inhibited which can be crucial for industrial waste heat flows. Multi-stage ORCs and the usage of a regenerator cause higher complexity and higher effort for measurement and control of the system. The thermal oil circuit normally used for high-temperature applications is excluded, instead, more efficient direct contact heaters are applied. In this study, a diaphragm pump covers the necessary broad range of absolute pressure and pressure ratio. Shell-and-tube heat exchangers withstand high temperature and pressure. Following the trend from ORC manufacturers and based on the relatively high volume flow ratio, a turbine is chosen as expander.

3.2. Selection of Working Fluids

Publications have shown that trends for the behavior of thermodynamic and constructional parameters can be observed within a chemical class of working fluids [2,50]. Hence, instead of single and random fluids, whole chemical classes of working fluids are investigated in this study: *n*-alkanes, alkylbenzenes, linear and cyclic siloxanes. As the investigated temperature range in this study is high compared to usual ORC applications, a conventional Rankine Cycle based on water may be promising as well. However, Shu et al. [62] showed that some organic working fluids in a high-temperature ORC can reach similar output power and electricity production costs as water does. However, they did not include personnel costs during operation. In some European countries (like Germany) conventional Rankine Cycle devices need 24 h a day surveillance compared to ORC units which can be remotely controlled with personnel costs of 3–5 h/week (Table A2). Furthermore, water has different other drawbacks like bigger size, necessary superheating and water-treatment systems [63]. Hence, we concentrate on the evaluating of the mentioned chemical classes of organic working fluids. Furthermore, typical low-temperature working fluids like synthetic refrigerants R245fa and others are excluded in this study as these fluids are not competitive in the high-temperature range.

Within the homologous series from *n*-pentane to *n*-dodecane, physico-chemical properties behave continuously as the number of methyl groups increases and so the van-der-Waals forces increase gradually. The working fluid can be adapted in an optimal manner to the heat source and *n*-alkanes are cheap working fluids. However, flammability issues require high safety measures. This is also true for alkylbenzenes. Linear and cyclic siloxanes are far less flammable. The regular structure of Si-O-Si bonds and methyl-groups leads to a continuous behavior of fluid properties which is comparable to *n*-alkanes. The specific evaporation enthalpy is lower for siloxanes than for *n*-alkanes. Comparing linear and cyclic siloxanes, cyclic siloxanes have higher critical temperatures due to their ring bonds. All chemical classes fulfill recent legislation concerning zero ODP and GWP less than 150 [64,65]. Thermodynamic properties and *T,s*-diagrams are shown in Appendixes A and C.

3.3. Boundary Conditions

Process simulation is carried out using AspenPlus© [66]. Hot air with 78 mole-% nitrogen, 21 mole-% oxygen, and 1 mole-% argon serves as heat source. The mass flow rate is fixed to 5 kg/s for the thermodynamic analysis. Constructional boundary conditions for turbomachinery and heat exchanger are given in Table 1. For the maximum pressure in subcritical mode of operation and the minimum temperature after the heater relative values based on the maximum entropy of the dew line are chosen [67]. Other boundary conditions are in accordance with typical values from literature.

The Peng-Robinson-Boston-Mathias (PR-BM) model is chosen among the 82 available equations of state that are implemented in AspenPlus©. It is based on the cubic Peng-Robinson equation of state [68]. The main advantages of the model are the available volume transformation for the liquid molar volume and the additional alpha function for the supercritical mode of operation (Boston-Mathias alpha function [69]).

The accuracy of the model is validated for the working fluids *n*-pentane and hexamethyldisiloxane by comparison with the work of Lai et al. [2] who applied the BACKONE equation of state [70] for hydrocarbons and the PC-SAFT equation of state [71] for siloxanes. The maximum relative deviation is 0.4% for the maximum temperature in the process, 2.1% for the volume flow rate at the outlet of the

turbine, 1.9% for the heat flow rate in the heater, 1.4% for the heat capacity flow rate and 2.0% for the thermal efficiency.

Table 1. Boundary conditions for process simulation.

Efficiencies	Value
isentropic, turbine	75%
mechanical, generator	95%
isentropic, pump	80%
electromechanical, pump	85%
Minimum Temperature Approach of Heat Exchangers	
heater	35 K
internal recuperator	10 K
condenser	10 K
Pressure and Temperature	
maximum pressure subcritical	$p(s_{max})$
minimum pressure supercritical	$1.02 \cdot p_{crit}$
maximum pressure supercritical	$1.30 \cdot p_{crit}$
minimum temperature after heater	$T(s_{max})$

3.4. Thermodynamic and Constructional Evaluation Parameters

Evaluation of thermodynamic and constructional analysis is based on the following parameters: the main thermodynamic parameter is the exergetic efficiency of the process which is directly proportional to the net power output of the cycle via the exergy of the heat source. The net power output is the absolute turbine power minus the power of the pump. The exergy of the heat source is calculated with regard to the dead state temperature $T_0 = 15 \text{ }^\circ\text{C}$:

$$\eta_{ex} = \frac{P_{net}}{\dot{E}_{HS}} = \frac{|P_t| - P_p}{\dot{m}_{HS} \times [h - h_0 - T_0 \times (s - s_0)]} \quad (1)$$

The heat exchangers are evaluated by the heat exchanger capacity which is the ratio of heat flux \dot{Q} and logarithmic mean temperature difference *LMTD*:

$$kA = \frac{\dot{Q}}{LMTD} = \frac{\dot{Q}}{\frac{\Delta T_2 - \Delta T_1}{\ln(\Delta T_2 / \Delta T_1)}} \quad (2)$$

ΔT_1 and ΔT_2 are the temperature differences at inlet and outlet of the heat exchanger. Assuming a constant heat exchange coefficient as a first estimation for all working fluids, the heat exchange capacity is proportional to the heat exchanger area and to its cost.

The turbine is described by three parameters. The size parameter *SP* according to Angelino et al. [72] accounts for the dimension of the turbine. It depends on the volume flow rate at the outlet of the turbine $\dot{V}_{out,t}$ and the isentropic enthalpy drop $\Delta h_{is,t}$:

$$SP = \frac{\sqrt{\dot{V}_{out,t}}}{\Delta h_{is,t}^{1/4}} \quad (3)$$

The volume flow ratio V_{ratio} between outlet and inlet is a measure for the complexity of the turbine:

$$V_{ratio} = \frac{\dot{V}_{out}}{\dot{V}_{in}} \quad (4)$$

Last, the rotational speed n is calculated based on the specific speed N_s defined by Angelino et al. [72] and has a value of $N_s = 0.10$ [73]:

$$n = \frac{\Delta h_{is,t}^{3/4} \cdot N_s}{\sqrt{\dot{V}_{out,t}}} \quad (5)$$

3.5. Overall Flow Chart

Different datasets have been used for the analyses in the following chapters. Figure 4 displays these datasets and summarizes the main results from each dataset to provide a guide through the results of Sections 4–6.

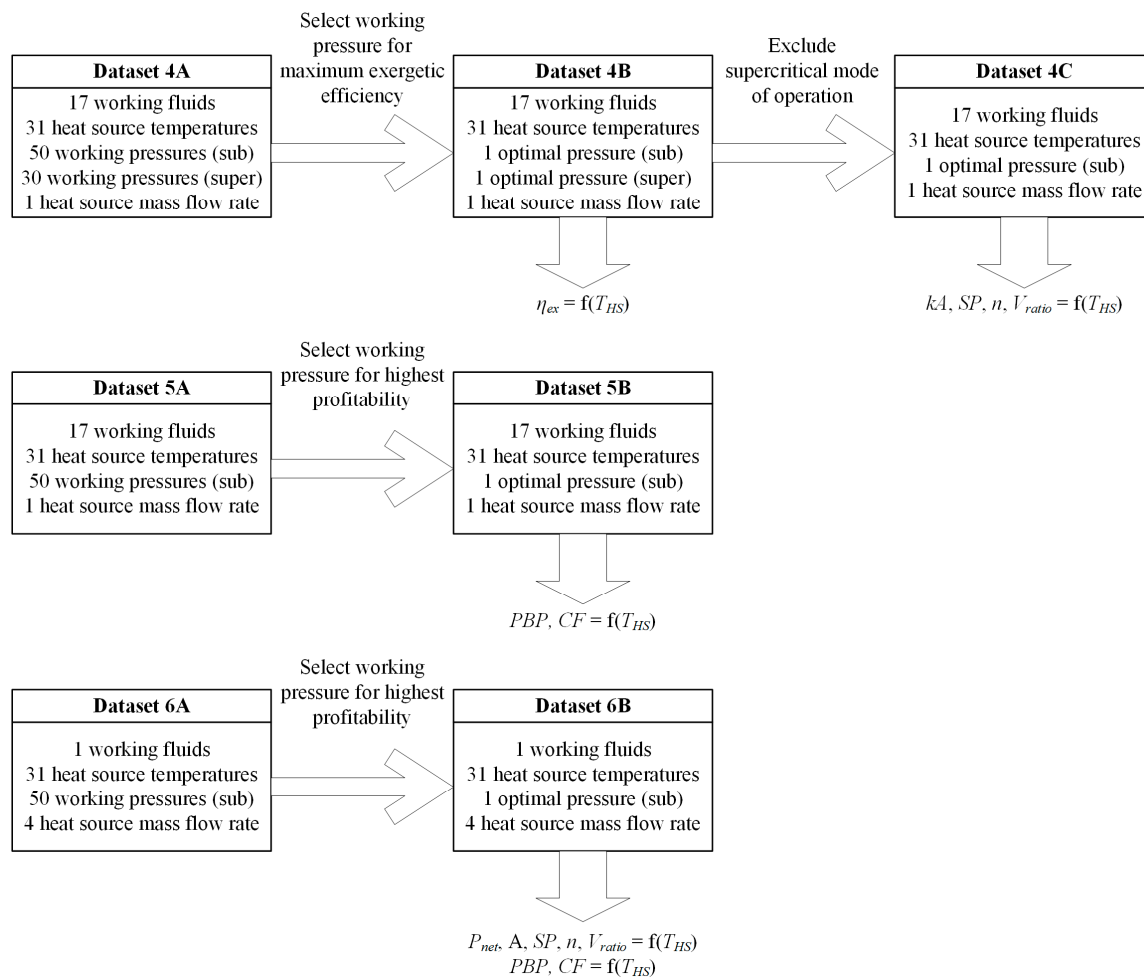


Figure 4. Overview of datasets (defined in Section 3.5) used in each chapter and results of related parameters (defined in Sections 3.4 and 5.2).

In Section 4, all 17 working fluids are simulated for 31 heat source temperatures, 50 subcritical and 30 supercritical working pressures within AspenPlus (see Section 3.3). The main goal is to analyze how thermodynamic and constructional parameters depend on heat source temperature. Therefore, the mass flow rate of the heat source is set to a constant value. By selecting the optimum working pressure for each fluid and heat source temperature, dataset 4B leads to the exergetic efficiency over the heat source temperature. After excluding the supercritical mode of operation, dataset 4C gives the result of constructional parameters.

Section 5 transforms the thermodynamic and constructional parameters into the economic indicators of payback period (*PBP*) and discounted cash flow (*CF*) via a self-made Matlab-tool but still based on the results from the AspenPlus simulation. For this purpose, the working pressure which leads to the highest profitability, not the one which leads to the highest exergetic efficiency, is selected

from dataset 5A. Subsequently, this leads to dataset 5C and the correlation between payback period, cash flow, and heat source temperature.

Finally, within Section 6, dataset 6A and 6B take the mass flow rate of the heat source into account to analyze the influence of the size of the ORC on the thermodynamic, constructional and economic parameters. In the end, dataset 6B leads to recommendations for a modular ORC design.

4. Thermodynamic and Constructional Evaluation

4.1. Thermodynamic Results

Thermodynamic process simulation for each of the selected fluids is the first step of the thermoeconomic analysis. The results for subcritical and supercritical mode of operation are displayed in Figure 5. For each heat source temperature, the most efficient working fluid among the chemical class is taken. For the homologous series of alkanes, a shift between one working fluid and the other occurs about every 50 to 60 K (in total six shifts occur). For supercritical mode of operation, the shift occurs about 10 to 20 K later. The other chemical classes show a similar trend with two shifts of the optimal working fluid within the investigated temperature range.

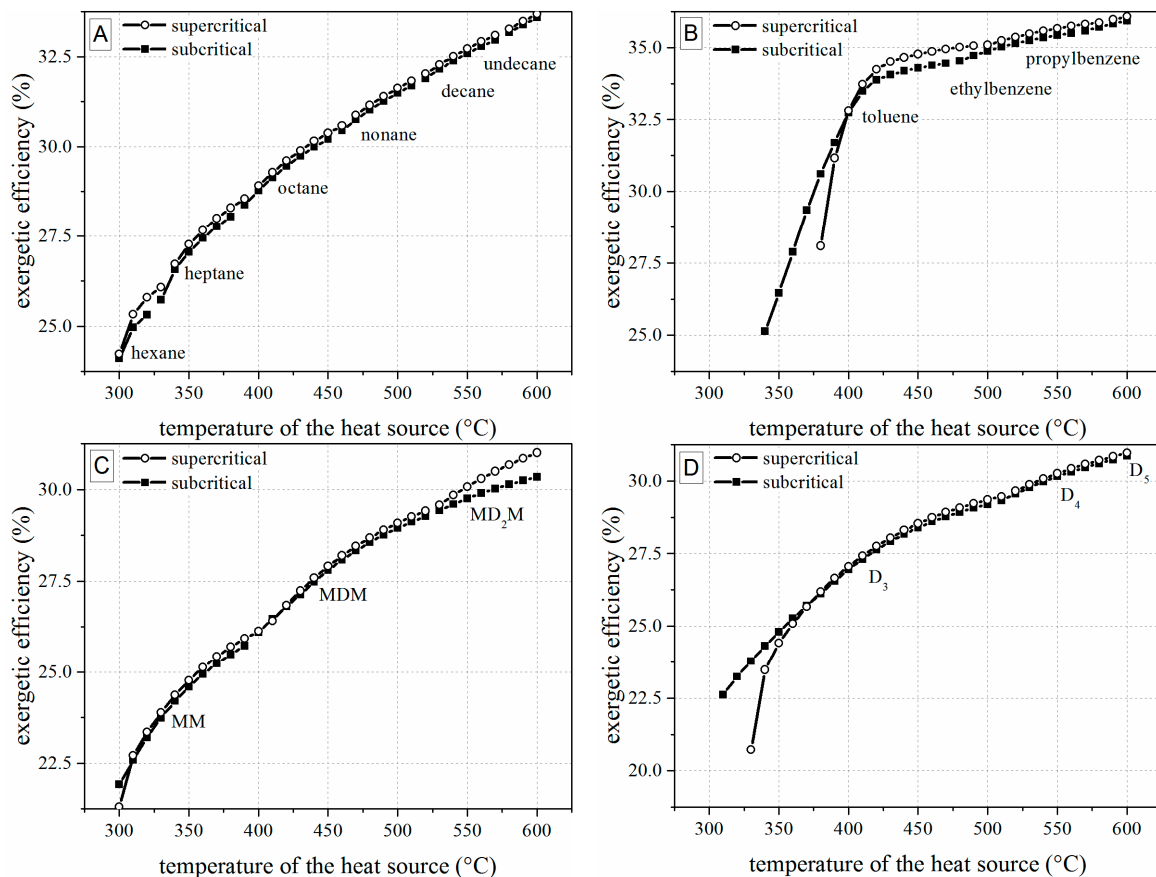


Figure 5. Exergetic efficiency for supercritical and subcritical mode of operation for varied heat source temperature ((A) *n*-alkanes; (B) alkylbenzenes; (C) linear siloxanes; and (D) cyclic siloxanes).

The general behavior can be explained by the location of the pinch point and by the fluid properties in Table A1 in the Appendix A. For an efficient operation, the heating curve of the working fluid must fit the cooling curve of the heat source to reach small mean temperature differences during heat transfer. Hence, the smaller the area between those two heat flows in a temperature/heat flux-diagram is, the lower are the exergy losses and the higher is the exergetic efficiency. If the critical temperature of

the working fluid is close to the heat source temperature or even higher, the pinch point for subcritical processes is located at the beginning of the evaporation and high exergy losses are observed during preheating. However, if the critical temperature is far lower than the heat source temperature, the pinch point is located at the beginning of the preheating and exergy losses during evaporation increase. For high-temperature applications and high reduced pressures p/p_{crit} , the system is most efficient if the preheating just shifts from evaporation to preheating (see Figure 6, middle). Therefore, the higher the heat source temperature, the higher the critical temperature of the working fluid must be for an efficient system. However, an optimal value which is valid for all chemical classes and, therefore, a rule like “the critical temperature always has to be X K below the heat source temperature” cannot be established as next to the critical temperature, the slope of the boiling point line also influences the location of the pinch point.

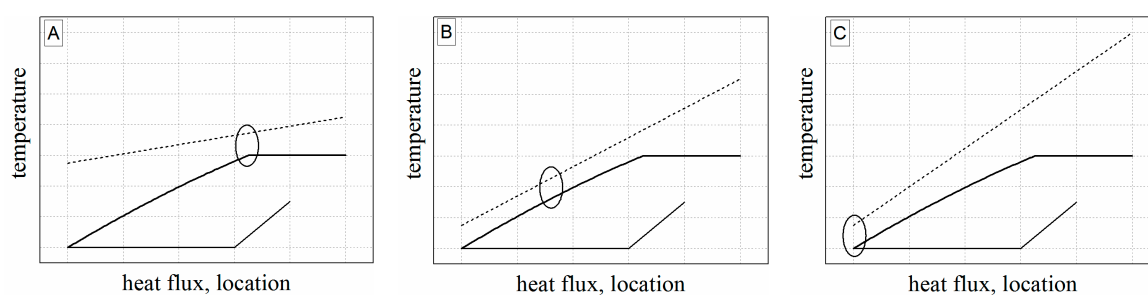


Figure 6. Temperature-heat flow-diagram (A) pinch point at beginning of evaporation; (B) pinch point during preheating; (C) pinch point beginning of preheating).

The maximum increase in efficiency for the supercritical mode of operation compared to the subcritical system is low (1.9% for *n*-alkanes, 1.1% for alkylbenzenes, 2.2% for linear siloxanes and 0.4% for cyclic siloxanes). As supercritical ORCs have higher requirements concerning constructional effort (high pressures) and heat exchanger design (dramatic change of fluid properties near the pseudocritical point), supercritical mode of operation is excluded at this stage of the study.

4.2. Analysis of Constructional Parameters

Next to the efficiency, constructional parameters for heat exchanger and turbine have to be taken into account. Figure 7 summarizes heat exchange capacity, volume flow ratio, size parameter and rotational speed of the most efficient working fluid for each heat source temperature. The change in the most efficient working fluid (see Figure 5) for each chemical class also cause a leap in the constructional parameters. The leap in the heat exchange capacity is small as the efficiency also depends on the heat input in the heater (available heat) and the logarithmic mean temperature difference (measure for the irreversibilities). Hence, as the exergetic efficiency increases gradually in Figure 5, the heat exchange capacity in Figure 7 does as well. The thermodynamic dependency between heat exchange capacity and exergetic efficiency also explains that alkylbenzenes have lower values than alkanes (+10%) and siloxanes (linear +31% and cyclic +27%). Compared to this steady behavior, the turbine parameters show a clear leap from one fluid to the other as the working pressure of the fluids differs significantly due to the deviating critical pressures. Although the volume flow ratio for temperatures lower than 380 °C is almost the same for all chemical classes, linear siloxanes show favorable behavior, especially for high heat source temperatures. Based on the definition in Equations (3) and (5), the size parameter and the rotational speed behave contrary. In average, linear siloxanes have 1.9 times larger turbines than alkylbenzenes but the latter have more complex turbines due to a 1.6 times higher rotational speed. Thermodynamic and constructional analysis can be shortly summarized as follows:

- Alkylbenzenes are favorable working fluids concerning exergetic efficiency, dimension of the turbine (SP) and heat exchanger (kA).

- Linear siloxanes have significant advantages concerning the complexity of the turbine due to low rotational speed.
- *n*-Alkanes combine the disadvantages of both formerly mentioned chemical classes.
- None of the chemical classes outperforms in all relevant parameters.

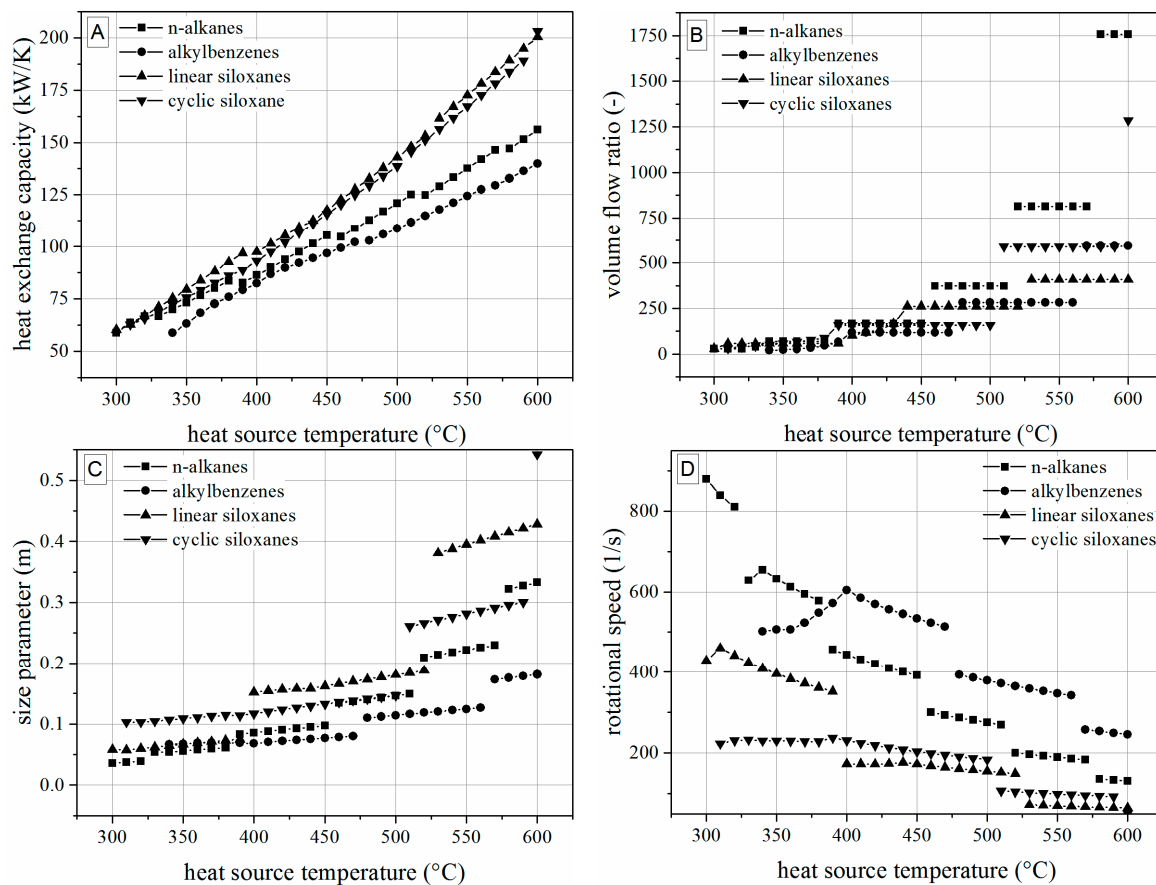


Figure 7. Heat exchange capacity (A), volume flow ratio (B), size parameter (C) and rotational speed (D) depending on the heat source temperature.

The last issue emphasizes the importance of a more sophisticated analysis in which thermodynamic and constructional parameters are correlated to economic behavior during the operational lifetime of an ORC. Hence, the following chapter investigates the chemical classes based on a thermoeconomic approach.

5. Thermoeconomic Evaluation

5.1. Thermoeconomic Modeling

Section 4 made clear that no chemical class of working fluids is advantageous in all thermodynamic and constructional aspects. Therefore, the specific parameters have to be weighted to allow a holistic approach. In this study, a thermodynamic and constructional model is developed and, subsequently, integrated into an economic analysis. The main elements and fundamentals of this model are presented and discussed in the following section, details can be found elsewhere [74].

The model is mainly based on the exponential dependency of investment cost I and capacity C , which was first introduced by Williams [10]:

$$\frac{I_i}{I_{i,ref}} = \left(\frac{C_i}{C_{i,ref}} \right)^m \quad (6)$$

The exponential factor m is specific for each component. In the denominator of the terms in Equation (6), the investment costs and the capacity of a reference plant have to be inserted. We used the direct costs of an existing ORC unit described by Obernberger et al. [75] compared to using absolute cost functions from the literature [76]. We converted the costs to the current price level by assuming an annual inflation of 2.3%. The total specific costs of the ORC then account for 2620 €/kW. The total costs are divided by the share of each component which is assumed to be 35% for the heat exchangers, 10% for the pump, 15% for the piping and 40% for the turbine-generator-unit [77–79]. For each component, a specific capacity has to be inserted into Equation (6) as follows.

5.1.1. Heat Exchanger

The capacity parameter of condenser, internal recuperator and evaporator is the area of the heat exchanger. Shell-and-tube heat exchangers (STHE) are used in this study due to the simple scaling for modular ORC units (increasing the number and/or length of the tubes) and the broad pressure and temperature range in which STHE can be applied. Plate heat exchangers which are commonly used in low-temperature and small-scale ORCs [63] are excluded due to limited stability in case of high-temperature differences compared to STHE which are also used for high temperatures in mobile ORCs [80]. The model in the one-phase region is based on the Nusselt correlation according to Gnielinski [81] whereas the correlation of Konakov [82] predicts the pipe friction factor ζ . K is a correction factor for the difference between the wall temperature and the bulk temperature:

$$\text{Nu} = \frac{(\zeta/8) \cdot \text{Re} \cdot \text{Pr}}{1 + 12.7 \cdot \sqrt{\zeta/8} \cdot (\text{Pr}^{2/3} - 1)} \cdot \left[1 + \left(\frac{d}{L} \right)^{2/3} \right] \cdot K \quad (7)$$

The evaporator is modeled with the approach of convective boiling, whereas the heat transfer coefficient α_x is related to the vapor fraction [83]:

$$\alpha_x = \left\{ \begin{array}{l} (1-x)^{0.01} \cdot \left[(1-x)^{1.5} + 1.2 \cdot x^{0.4} \cdot R^{0.37} \right]^{-2.2} \\ + x^{0.01} \cdot \left[\frac{\alpha_{g0}}{\alpha_{l0}} (1 + 8 \cdot (1-x)^{0.7} \cdot R^{0.67}) \right]^{-2} \end{array} \right\}^{-0.5} \cdot \alpha_{l0} \quad (8)$$

R is defined as the ratio between liquid and gas density, α_{g0} is the heat transfer coefficient of the gas phase and α_{l0} of the liquid phase according to Equation (7).

The correlation of Shah [84] describes the local Nusselt number for each vapor quality in the condenser with p_r being the reduced pressure p/p_{crit} :

$$\text{Nu} = 0.023 \text{Re}^{0.8} \cdot \text{Pr}^{0.4} \cdot \left\{ (1-x)^{0.8} + \frac{3.8(1-x)^{0.04} x^{0.76}}{p_r^{0.38}} \right\} \quad (9)$$

Subsequently, the heat exchanger area is calculated by using the NTU of an ideal countercurrent heat exchanger (index i,c) and applying the correction factor F based on Roetzel and Spang [85] for one outer and two inner passes in the shell (a, b, c, d are fit parameters):

$$F = \frac{NTU_{i,c}}{NTU} = \frac{1}{(1 + aR_i^{db} NTU_i^b)^c}, \quad i = 1, 2 \quad (10)$$

$$A = \frac{NTU_i \cdot \dot{Q}_i}{k}, \quad i = 1, 2 \quad (11)$$

\dot{Q} is heat flux and k overall heat transfer coefficient. Exponential factor m for STHE is 0.59 [86].

5.1.2. Pump

The power of the pump is inserted as capacity factor and m is set to 0.43 [87].

5.1.3. Turbine

For the turbine, a more complex model is developed as in the literature the exponential factor m is just available for large-scale steam turbines, however, not for small- to medium-scale ORC turbines. Most models focus on the size of the turbine, not on its complexity [73,88] or use the mentioned cost functions for steam turbines [89,90]. The newly developed model aims to account for both, the size and also the complexity of the turbine and to be ORC specific. Furthermore, turbine and generator are defined as one constructional combined assembly, the turbine-generator-unit (TGU). This approach reduces the investment costs, increases the efficiency and especially matters for a power output of less than 500 kW. Some ORC manufacturers already offer such systems successfully on the market [91,92]. Second, the investment costs for the TGU are subdivided into three main cost types: material input and processing, bearings and engineering. The share is chosen to 70%, 20%, and 10%. Each of the cost types is correlated with a constructional parameter: material costs depend on the size of the turbine and, therefore, on the size parameter (Equation (3)); costs of bearing and engineering are complexity parameters correlated to the rotational speed of the turbine (Equation (5)). The share of each cost type and the exponential factors within Equation (12) are chosen based on intensive discussions with turbine manufacturers:

$$\frac{I_{TGU}}{I_{TGU,ref}} = \left[0.7 \cdot \left(\frac{SP_t}{SP_{t,ref}} \right)^{2.5} + 0.1 \cdot \left(\frac{n_t}{n_{t,ref}} \right)^{1.5} + 0.2 \cdot \left(\frac{n_t}{n_{t,ref}} \right)^{1.5} \right] \quad (12)$$

As Equation (12) is based on continuous functions, it still does not account for technology leaps. However, such leaps can increase the investment costs of TGU tremendously when constructional parameters reach specific values. For TGU in ORC systems, the turning point between one-stage turbines and two-stage turbines is between a volume flow ratio of 50 and 220 [92–96]. In this study, we increase the investment costs of the TGU by 25% if the value exceeds a conservative mean value of 100. Furthermore, the costs for the bearings increase dramatically for rotational speeds of more than 30,000 revolutions/min as expensive magnetic bearings have to be used instead of cheap ball bearings. Hence, the costs of the TGU are increased by a factor of 1.9 in such cases:

$$I_{TGU} = \begin{cases} I_{TGU} \cdot 1.25 & \text{for } V_{Ratio} > 100 \\ I_{TGU} \cdot 1.90 & \text{for } n > 30,000 \frac{1}{\text{min}} \end{cases} \quad (13)$$

5.1.4. Piping

The piping is scaled based on the diameter of the pipes with an exponential factor of 1.33 [86].

5.2. Thermo-economic Results

The exergetic efficiency of Figure 5 and the constructional parameters of Figure 7 are transformed by the equations of Section 5.1 into economic indicators. Figure 8 shows exemplarily the payback period (PBP) and the discounted cash flow (CF) after operating time for different heat source temperatures. Main boundary conditions for the economic analysis are given in Table A2 in the Appendix B. Due to low-rate environment at the moment, the study is based on 100% share of loan capital with an interest rate of 4%. Note that a 4% discount factor is an example which is used for the economic computation. Higher values would lead to correspondingly higher PBP and lower CF.

The observed change of the most efficient working fluid every 50 to 60 K is not valid anymore if the economic behavior is analyzed. Among n -alkanes, n -heptane is most valuable in terms of cash flow up to 330 °C, n -nonane from 360 °C to 440 °C and n -octane at all other heat source temperatures.

For the linear siloxanes, MDM has to be chosen from an economic point of view within the temperature range of 330 °C to 430 °C, otherwise, MM is advantageous. The difference between MM and MDM, however, is small. MDM has higher net power output for temperatures above 390 °C and has lower rotational speeds of the turbine. Due to the higher evaporation enthalpy (see T,s -diagram in Figure A1), MM leads to lower heat exchanger area. Furthermore, the volume flow ratio and the dimension of the turbine are lower. This overcompensates the lower power output above 430 °C.

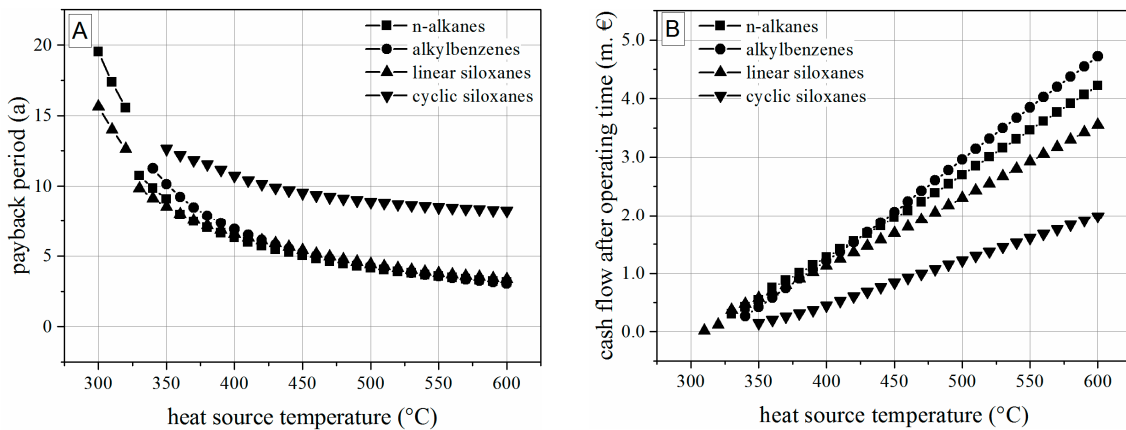


Figure 8. Payback period (A) in years and cash flow (B) in million € for all four chemical classes depending on heat source temperature.

Section 5.2 can be summarized as follows: considering thermoeconomic criteria and optimizing economic indicators, the number of advantageous working fluids decreases compared to the optimized net power output approach. Furthermore, the difference between two working fluids which seem to be significant in terms of exergetic efficiency and, therefore, net power output, may be neglected from an economic point of view. Same is true if we compare different chemical classes. Although alkylbenzenes and alkanes have higher exergetic efficiencies, siloxanes reach a similar payback period with a slightly lower cash flow due to favorable constructional parameters. Due to lower safety requirements of siloxanes, their thermal stability [97] and the broad knowledge in biomass fired power plants, siloxanes seem to be a promising chemical class for high-temperature ORC applications. Hence, the following chapter aims to derive a modular based ORC system for a broad range of heat source temperatures and mass flow rates by applying just one working fluid from one chemical class instead of adapting the working fluid to the heat source temperature. MM is chosen for this purpose.

6. Modularly-Designed ORC

To derive recommendations for modularly-designed ORC systems, the boundary condition of a constant mass flow rate of the heat source is neglected in this section. Hence, next to heat source temperature the mass flow rate is also varied for sensitivity purposes. Figures 9–14 show in each combination of heat source temperature and mass flow rate the thermodynamic state point of MM, i.e., the working pressure of MM, which leads to the highest cash flow of the power plant. As expected, the net power output and the heat exchanger area increase gradually with increasing heat source temperature and mass flow rate. This behavior is beneficial for a modular concept of ORC systems as the chosen shell-and-tube heat exchangers can also be adapted gradually by increasing the number or length of the pipes. The turbine parameters, however, behave differently. As the maximum cash flow is reached at working pressures lower than the maximum pressure for heat source temperature below 400 °C, an unsteady behavior of rotational speed, volume flow ratio, and size parameter is observed at this point. If one increases the heat source temperature further the maximum cash flow is always reached at the highest possible working pressure of 17.4 bar. The pressure is constant and the turbine parameters become steady as well. To summarize, a modular concept for ORC systems based

on MM as working fluid is favorable for the temperature range of 400 °C to 600 °C. In this temperature range, the working pressure remains constant. Hence, the design of the ORC components remains unchanged, just the size must be adapted. This leads to lower cost of development and engineering and, therefore, to more profitable units.

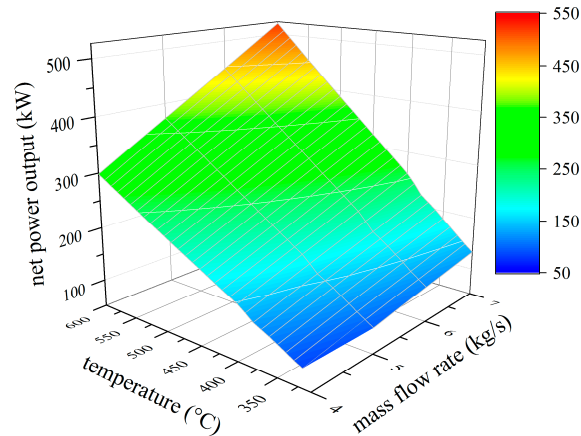


Figure 9. Net power output of hexamethyldisiloxane depending on heat source temperature and mass flow rate.

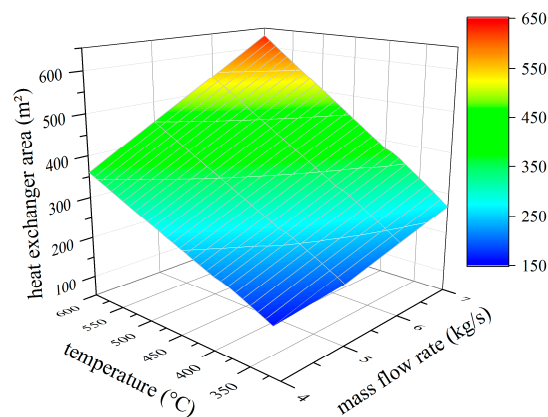


Figure 10. Heat exchanger area of hexamethyldisiloxane depending on heat source temperature and mass flow rate.

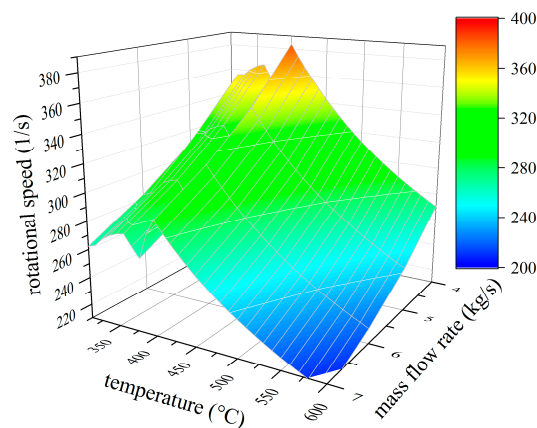


Figure 11. Turbine rotational speed of hexamethyldisiloxane depending on heat source temperature and mass flow rate.

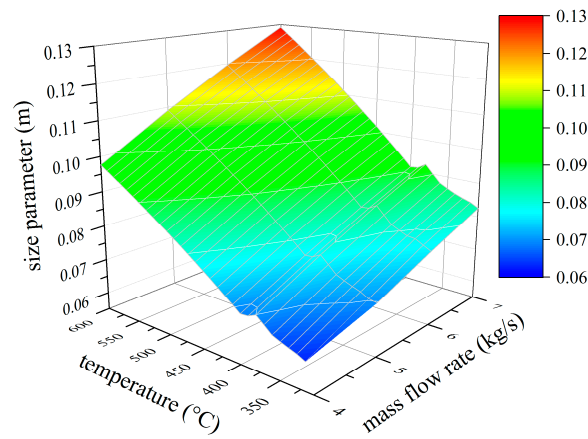


Figure 12. Size parameter of hexamethyldisiloxane depending on heat source temperature and mass flow rate.

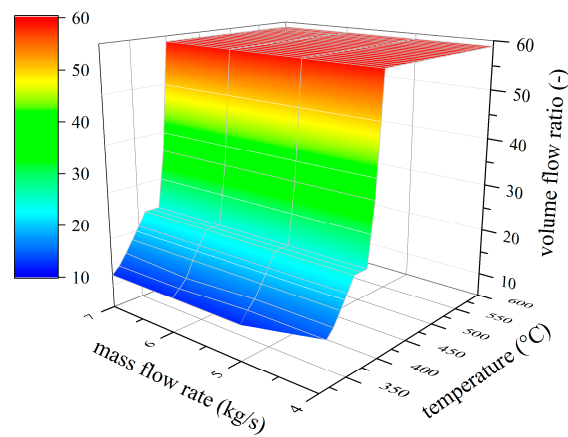


Figure 13. Volume flow ratio of hexamethyldisiloxane depending on heat source temperature and mass flow rate.

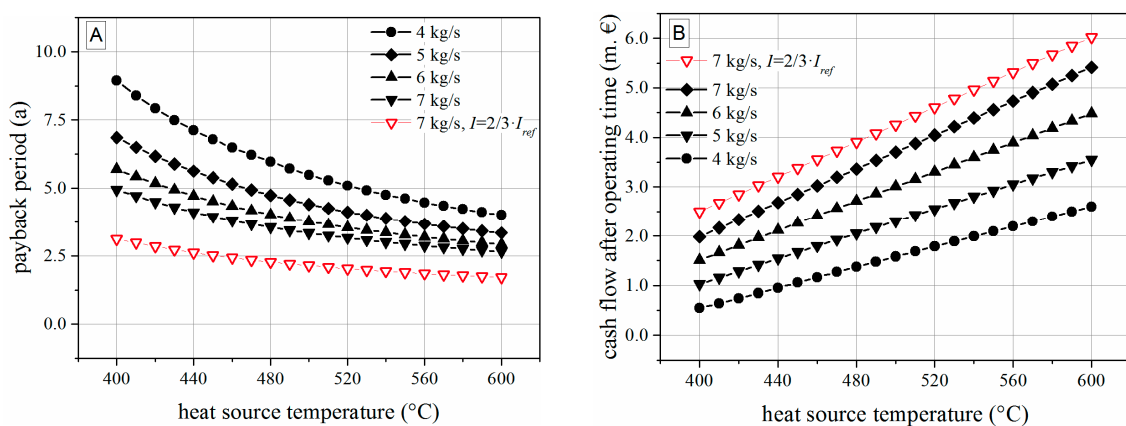


Figure 14. Payback period (A) in years and cash flow (B) in million € after operating time for hexamethyldisiloxane at different mass flow rates (red and hollow triangles: assumption of reduced investment costs).

7. Conclusions

Four different chemical classes of working fluids were investigated for high-temperature industrial waste heat recovery based on the Organic Rankine Cycle (ORC). A thermoeconomic approach was applied and modularly-designed ORC systems were evaluated. The research questions from the introduction can be answered as follows:

1. Taking into account thermodynamic, construction and economic parameters, linear siloxanes and within this group, the working fluid hexamethyldisiloxane is a promising candidate for waste heat recovery in a broad range of heat source temperatures and capacities.
2. A concept with direct contact evaporator, internal recuperator, and expansion by a turbine is a favorable design for modularly-based ORC units.
3. A holistic thermoeconomic approach has to be based on scaling and complexity parameters. Especially for the turbine, the typically used exponential cost estimation method is not appropriate as technology leaps can occur depending on the working pressure.
4. For the boundary conditions and turbine model within this study, a modular concept based on hexamethyldisiloxane, a temperature range of 400 to 600 °C and a mass flow rate exceeding 4 kg/s can be recommended.

Future work will include experimental evaluation of ORC turbines and direct contact heat exchangers in the newly built test field of our Center of Energy Technology at the University of Bayreuth. Hence, it will be possible to investigate the approach within this study from an experimental point of view. Furthermore, as the thermoeconomic model is implemented in Matlab, the adaption to different ORC design and related cost function, e.g., for scroll expanders, is possible.

Acknowledgments: The authors gratefully acknowledge financial support of the Bayerische Staatsministerium für Bildung und Kultus, Wissenschaft und Kunst within the framework “Kompetenzzentrum Kraft-Wärme-Kopplung”.

Author Contributions: All authors contributed to this work by collaboration. Markus Preißinger is the main author of this manuscript. Dieter Brüggemann supervised the project. All authors revised and approved the publication.

Conflicts of Interest: The authors declare no conflict of interest.

Nomenclature

Abbreviations

a	year
CF	Cash flow
D ₃	hexamethylcyclotrisiloxane
D ₄	octamethylcyclotetrasiloxane
D ₅	decamethylcyclopentasiloxane
MD ₂ M	decamethyltetrasiloxane
MDM	octamethyltrisiloxane
MM	hexamethyldisiloxane
O	oxygen
ORC	Organic Rankine Cycle
P	plant
PBP	payback period
PR-BM	Peng-Robinson Boston-Mathias
Ref	reference plant
Si	silicium
STHE	shell-and-tube heat exchanger
sub	subcritical
super	supercritical

Subscripts

0	dead state
c	countercurrent
crit	critical
ex	exergetic
g	gaseous
HS	heat source
i	component i
is	isentropic
l	liquid
max	maximum
P	pump
r	reduced
s	specific
s	saturation
t	turbine
TGU	turbine-generator-unit

Symbols

		Unit
T	temperature	$^{\circ}\text{C}, \text{K}$
A	heat exchanger area	m^2
C	capacity	W, m^2
D	diameter	m
F	correction factor	-
h	specific enthalpy	kJ/kg
I	investment costs	€
kA	heat exchanger capacity	W/m^2
L	length	m
$LMTD$	logarithmic mean temperature difference	K
M	exponential factor	-
M	molar mass	g/mol
\dot{m}	mass flow rate	kg/s
n	rotational speed	$1/\text{s}$
NTU	number of transfer units	-
Nu	Nusselt number	-
Pr	Prandl number	-
\dot{Q}	heat flux	W
R	density ratio	-
Re	Reynolds number	-
s	specific entropy	kJ/kgK
SP	size parameter	M
\dot{V}	volume flow rate	m^3/s
x	vapor fraction	-
Greek symbols		
η	efficiency	
ζ	pipe friction factor	

Appendix A Physico-Chemical Properties of Evaluated Working Fluids**Table A1.** Molar mass M , saturation temperature T_s at 1 bar, saturation pressure p_s at 85°C , critical temperature T_{crit} and pressure p_{crit} for evaluated working fluids.

Name	Abbreviation	M	T_s (1 bar)	p_s (85°C)	T_{crit}	p_{crit}
		g/mol	K	bar	K	bar
<i>n</i> -pentane		72.15	309.22	4.16	469.70	33.70
<i>n</i> -hexane		86.18	341.88	1.63	507.60	30.25
<i>n</i> -heptane		100.20	371.58	0.67	540.20	27.40
<i>n</i> -octane		114.23	398.83	0.28	568.70	24.90

Table A1. Cont.

Name	Abbreviation	M g/mol	T_s (1 bar) K	p_s (85 °C) bar	T_{crit} K	p_{crit} bar
<i>n</i> -nonane		128.26	423.97	0.12	594.60	22.90
<i>n</i> -decane		142.28	447.30	0.05	617.70	21.10
<i>n</i> -undecane		156.31	469.08	0.02	639.00	19.50
<i>n</i> -dodecane		170.34	489.48	0.01	658.00	18.20
methylbenzene	toluene	92.14	383.78	0.46	591.75	41.08
ethylbenzene		106.17	409.35	0.20	617.15	36.09
<i>n</i> -propylbenzene		120.19	432.39	0.10	638.35	32.00
hexamethyldisiloxane	MM	162.38	373.67	0.63	518.70	19.14
octamethyltrisiloxane	MDM	236.53	425.70	0.12	564.40	14.40
decamethyltetrasiloxane	MD ₂ M	310.69	467.50	0.02	599.40	12.27
hexamethylcyclotrisiloxane	D ₃	222.46	408.26	0.21	554.20	16.63
octamethylcyclotetrasiloxane	D ₄	296.62	448.15	0.05	586.50	13.32
decamethylcyclopentasiloxane	D ₅	307.77	484.10	0.01	619.15	11.60

Appendix B Boundary Conditions for Economic Evaluation

Table A2. Boundary conditions for economic analysis.

Parameter	Value	Unit	Reference
operational life time	20	a	
full load hours	8000	h/a	
price of electricity	12.88	€-Cent/kWh	[98]
ancillary costs	35	% of invest	[28]
specific cost of cooling	0.1288	€-Cent/kWh _{th}	[28,99,100]
specific cost of maintenance	2.0	% of invest per year	[99]
specific cost of insurance	2.0	% of invest per year	[101]
specific cost of process integration	20	% of invest	[101]
specific cost of personnel	40	€/h	
working hours of personnel	260	h/year	[75]
inflation electricity	4.0	%	
inflation general	2.0	%	
tax rate	28.8	%	
interest rate	4.0	%	
share of loan capital	100	%	
redemption time	20	a	
redemption rate	5.0	%	

Appendix C Temperature-Entropy-Diagrams of the Investigated Working Fluids

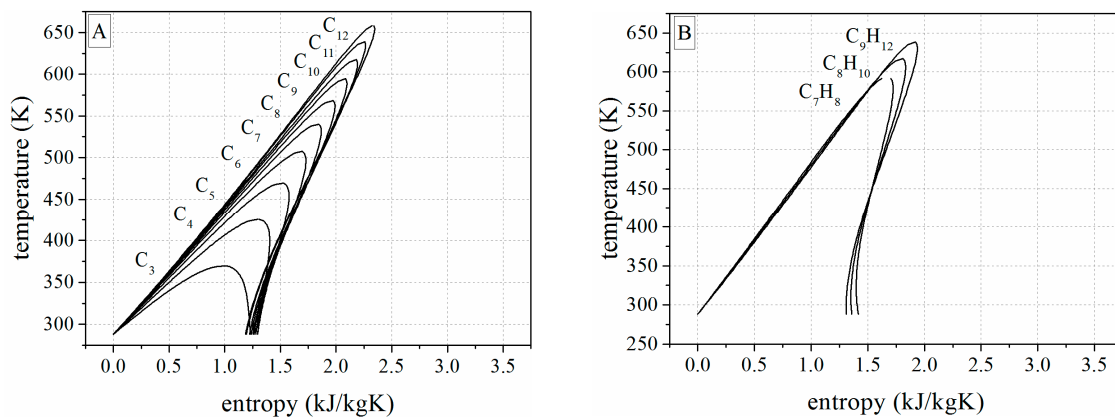


Figure A1. Cont.

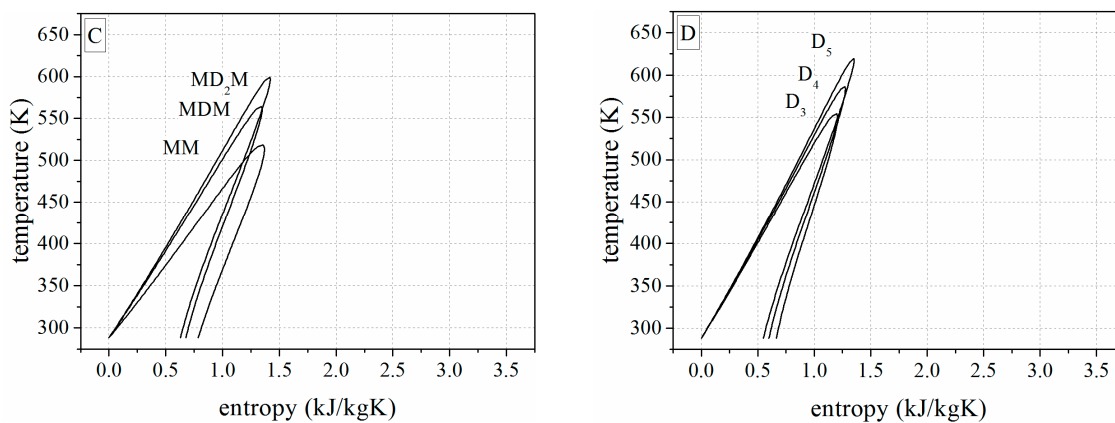


Figure A1. *T*-*s*-diagrams of investigated working fluids (A) *n*-alkanes; (B) alkylbenzenes; (C) linear siloxanes; and (D) cyclic siloxanes.

References

1. European Union. *Directive 2006/32/EC of the European Parliament and the Council on Energy End-Use Efficiency and Energy Services and Repealing Council Directive 93/76/EEC*; European Union: Brussels, Belgium, 2006.
2. Lai, N.A.; Wendland, M.; Fischer, J. Working fluids for high-temperature organic Rankine cycles. *Energy* **2011**, *36*, 199–211. [[CrossRef](#)]
3. Drescher, U.; Brüggemann, D. Fluid selection for the Organic Rankine Cycle (ORC) in biomass power and heat plants. *Appl. Therm. Eng.* **2007**, *27*, 223–228. [[CrossRef](#)]
4. Saleh, B.; Koglbauer, G.; Wendland, M.; Fischer, J. Working fluids for low-temperature Organic Rankine Cycles. *Energy* **2007**, *32*, 1210–1221. [[CrossRef](#)]
5. Bao, J.; Zhao, L. A review of working fluid and expander selections for Organic Rankine Cycle. *Renew. Sustain. Energy Rev.* **2013**, *24*, 325–342. [[CrossRef](#)]
6. Linke, P.; Papadopoulos, A.; Seferlis, P. Systematic Methods for Working Fluid Selection and the Design, Integration and Control of Organic Rankine Cycles—A Review. *Energies* **2015**, *8*, 4755–4801. [[CrossRef](#)]
7. Schwöbel, J.A.H.; Preißinger, M.; Brüggemann, D.; Klamt, A. High-Throughput-Screening of Working Fluids for the Organic Rankine Cycle (ORC) based on COSMO-RS and Thermodynamic Process Simulations. *Ind. Eng. Chem. Res.* **2016**. [[CrossRef](#)]
8. Preißinger, M.; Schwöbel, J.; Klamt, A.; Brüggemann, D. High-Throughput Screening of ORC Fluids for Mobile Applications. In *Energy and Thermal Management, Air Conditioning, Waste Heat Recovery*; Junior, C., Jänsch, D., Dingel, O., Eds.; Springer International Publishing: Cham, Switzerland, 2017; pp. 35–40.
9. Preißinger, M.; Schatz, S.; Vogl, A.; König-Haagen, A.; Brüggemann, D. Thermo-economic analysis of configuration methods for modular Organic Rankine Cycle units in low-temperature applications. *Energy Convers. Manag.* **2016**, *127*, 25–34. [[CrossRef](#)]
10. Williams, R., Jr. “Six-Tenths Factor” Aids in Approximating Costs. *Chem. Eng.* **1947**, *12*, 124–125.
11. Chilton, C. Six Tenths Factor applies to complete plant costs. *Chem. Eng.* **1950**, *57*, 112–114.
12. Lecompte, S.; Huisseune, H.; van den Broek, M.; Vanslambrouck, B.; de Paepe, M. Review of Organic Rankine Cycle (ORC) architectures for waste heat recovery. *Renew. Sustain. Energy Rev.* **2015**, *47*, 448–461. [[CrossRef](#)]
13. Colonna, P.; Casati, E.; Trapp, C.; Mathijssen, T.; Larjola, J.; Turunen-Saaresti, T.; Uusitalo, A. Organic Rankine Cycle Power Systems: From the Concept to Current Technology, Applications, and an Outlook to the Future. *J. Eng. Gas Turbines Power* **2015**, *137*, 100801–100819. [[CrossRef](#)]
14. Sollesnes, G.; Helgerud, H.E. *Utnyttelse av Spillvarme fra Norsk Industri—En Potensialstudie*; Enova: Trondheim, Norway, 2009. (In Norwegian)
15. Pehnt, M.; Bödeker, J.; Arens, M.; Jochem, E. *Die Nutzung Industrieller Abwärme—Technisch-Wirtschaftliche Potenziale und Energiepolitische Umsetzung*. Ifeu: Heidelberg, Germany, 2010. Available online: http://www.isi.fraunhofer.de/isi-wAssets/docs/e/de/publikationen/Nutzung_industrieller_Abwaerme.pdf (accessed on 20 December 2016). (In German)

16. iZES gmbH. Erschließung von Minderungspotenzialen Spezifischer Akteure, Instrumente und Technologien zur Erreichung der Klimaschutzziele im Rahmen der Nationalen Klimaschutzinitiative (EMSAITEK), Endbericht zu PART III Beitrag von Mini-KWK-Anlagen zur Zielerreichung der Nationalen Klimaschutzinitiative. Available online: www.izes.de/cms/upload/publikationen/EM_9_40_Teil_3.pdf (accessed on 17 July 2013).
17. Hamm, H.; Noeres, P.; Oser, E. Potenziale zur Nutzung von Abwärme für die Stromerzeugung. *Euroheat Power* **2008**, *37*, 36–43.
18. Berger, H.; Hoenig, V. *Energieeffizienz der Österreichischen Zementindustrie*; Vereinigung der Österreichischen Zementindustrie: Vienna, Austria, 2010.
19. Bailey, O.; Worrell, E. *Clean Energy Technologies: A Preliminary Inventory of the Potential for Electricity Generation*; University of California: Berkeley, CA, USA, 2005.
20. Galanis, N.; Cayer, E.; Roy, P.; Denis, E.; Désilets, M. Electricity Generation from Low Temperature Sources. *J. Appl. Fluid Mech.* **2009**, *2*, 55–67.
21. Zhang, L. Waste Heat Recovery from Metal Industries. *JOM* **2012**, *64*, 982–984. [[CrossRef](#)]
22. U.S. Department of Energy. *Waste Heat Recovery: Technology and Opportunities in U.S. Industry*; U.S. Department of Energy: Washington, DC, USA, 2008.
23. McKenna, R.; Norman, J. Spatial modelling of industrial heat loads and recovery potentials in the UK. *Energy Policy* **2010**, *38*, 5878–5891. [[CrossRef](#)]
24. Campana, F.; Bianchi, M.; Branchini, L.; de Pascale, A.; Peretto, A.; Baresi, M.; Fermi, A.; Rossetti, N.; Vescovo, R. ORC waste heat recovery in European energy intensive industries: Energy and GHG savings. *Energy Convers. Manag.* **2013**, *76*, 244–252. [[CrossRef](#)]
25. Schroeder, D.J. Organic Rankine Cycle Working Fluid Considerations for Waste Heat to Power Applications. *ASHRAE Trans.* **2010**, *116*, 525–533.
26. Obernberger, I.; Thornhofer, P.; Reisenhofer, E. Description and evaluation of the new 1000 kWel organic Rankine cycle process integrated in the biomass CHP plant in Lienz, Austria. *Euroheat Power* **2002**, *10*, 18–25.
27. Obernberger, I. Decentralized biomass combustion: State of the art and future development: Paper to the keynote lecture of the session “Processes for decentralized heat and power production based on combustion” at the 9th European Bioenergy Conference, June 1996, Copenhagen, Denmark. *Biomass Bioenergy* **1998**, *14*, 33–56.
28. Baatz, E.; Heidt, G. First waste heat power generating plant using the Organic Rankine Cycle Process for utilizing residual clinker cooler exhaust air: Erstes Abwärmekraftwerk nach dem Organic-Rankine-Cycle-Verfahren für die Restnutzung der Klinkerkühlerabluft. *Int. Cem.-Lime-Gypsum* **2000**, *8*, 425–436.
29. Schuster, A.; Karellas, S.; Kakaras, E.; Spliethoff, H. Energetic and economic investigation of Organic Rankine Cycle applications. *Appl. Therm. Eng.* **2009**, *29*, 1809–1817. [[CrossRef](#)]
30. Lemort, V.; Quoilin, S.; Cuevas, C.; Lebrun, J. Testing and modeling a scroll expander integrated into an Organic Rankine Cycle. *Appl. Therm. Eng.* **2009**, *29*, 3094–3102. [[CrossRef](#)]
31. Quoilin, S.; Lemort, V.; Lebrun, J. Experimental study and modeling of an Organic Rankine Cycle using scroll expander. *Appl. Energy* **2010**, *87*, 1260–1268. [[CrossRef](#)]
32. Leibowitz, H.; Smith, I.K.; Stosic, N. Cost Effective Small Scale ORC Systems for Power Recovery from Low Grade Heat Sources. In Proceedings of the ASME Advanced Energy Systems Division—2006, Chicago, IL, USA, 5–10 November 2006.
33. Smith, I.K.; Stosic, N.; Kovacevic, A. Screw expanders increase output and decrease the cost of geothermal binary power plant systems. In Proceedings of the Geothermal Resources Council Annual Meeting 2005: Geothermal Energy—The World’s Buried Treasure, Reno, NV, USA, 25–28 September 2005.
34. Brasz, J.; Biederman, B. Power Generation with a Centrifugal Compressor. U.S. Patent WO/2004/043607, 12 December 2004.
35. Brasz, J.; Biederman, B.; Holdmann, G. Power production from a moderate-temperature geothermal resource. In Proceedings of the Geothermal Resources Council Annual Meeting 2005: Geothermal Energy—The World’s Buried Treasure, Reno, NV, USA, 25–28 September 2005.
36. Klonowicz, P.; Borsukiewicz-Gozdur, A.; Hanausek, P.; Kryłłowicz, W.; Brüggemann, D. Design and performance measurements of an organic vapour turbine. *Appl. Therm. Eng.* **2014**, *63*, 297–303. [[CrossRef](#)]

37. Klonowicz, P.; Heberle, F.; Preißinger, M.; Brüggemann, D. Significance of loss correlations in performance prediction of small scale, highly loaded turbine stages working in Organic Rankine Cycles. *Energy* **2014**, *72*, 322–330. [[CrossRef](#)]
38. Angelino, G.; Di Colonna Paliano, P. Air cooled siloxane bottoming cycle for molten carbonate fuel cells. In Proceedings of the Fuel Cell Seminar, Portland, OR, USA, 30 October–2 November 2000.
39. Borsukiewicz-Gozdur, A. Influence of heat recuperation in ORC power plant on efficiency of waste heat utilization. *Arch. Thermodyn.* **2010**. [[CrossRef](#)]
40. Fernández, F.; Prieto, M.; Suárez, I. Thermodynamic analysis of high-temperature regenerative organic Rankine cycles using siloxanes as working fluids. *Energy* **2011**, *36*, 5239–5249. [[CrossRef](#)]
41. Schuster, A.; Karl, J.; Karellas, S. Simulation of an Innovative Stand-Alone Solar Desalination System Using an Organic Rankine Cycle. *Int. J. Thermodyn.* **2007**, *10*, 155–163.
42. Desai, N.B.; Bandyopadhyay, S. Process integration of organic Rankine cycle. *Energy* **2009**, *34*, 1674–1686. [[CrossRef](#)]
43. Yari, M. Exergetic analysis of various types of geothermal power plants. *Renew. Energy* **2010**, *35*, 112–121. [[CrossRef](#)]
44. Ayachi, F.; Ksayer, E.; Mazet, N.; Neveu, P.; Zoughaib, A.; Cardon, G. ORC system performances for medium grade heat recovery. In Proceedings of the Heat Powered Cycles 2012, Alkmaar, The Netherlands, 10–12 September 2012.
45. Habka, M.; Ajib, S. Investigation of novel, hybrid, geothermal-energized cogeneration plants based on organic Rankine cycle. *Energy* **2014**, *70*, 212–222. [[CrossRef](#)]
46. Kane, M. Small hybrid solar power system. *Energy* **2003**, *28*, 1427–1443. [[CrossRef](#)]
47. Kosmadakis, G.; Manolakos, D.; Kyritsis, S.; Papadakis, G. Comparative thermodynamic study of refrigerants to select the best for use in the high-temperature stage of a two-stage organic Rankine cycle for RO desalination. *Desalination* **2009**, *243*, 74–94. [[CrossRef](#)]
48. Kosmadakis, G.; Manolakos, D.; Papadakis, G. Parametric theoretical study of a two-stage solar organic Rankine cycle for RO desalination. *Renew. Energy* **2010**, *35*, 989–996. [[CrossRef](#)]
49. Meinel, D.; Wieland, C.; Spliethoff, H. Effect and comparison of different working fluids on a two-stage organic rankine cycle (ORC) concept. *Appl. Therm. Eng.* **2014**, *63*, 246–253. [[CrossRef](#)]
50. Preißinger, M.; Heberle, F.; Brüggemann, D. Thermodynamic analysis of double-stage biomass fired Organic Rankine Cycle for micro-cogeneration. *Int. J. Energy Res.* **2012**, *36*, 989–996. [[CrossRef](#)]
51. Romeo, L.M.; Lara, Y.; González, A. Reducing energy penalties in carbon capture with Organic Rankine Cycles. *Appl. Therm. Eng.* **2011**, *31*, 2928–2935. [[CrossRef](#)]
52. Stijepovic, M.Z.; Papadopoulos, A.I.; Linke, P.; Grujic, A.S.; Seferlis, P. An exergy composite curves approach for the design of optimum multi-pressure organic Rankine cycle processes. *Energy* **2014**, *69*, 285–298. [[CrossRef](#)]
53. Angelino, G.; Colonna, P. Multicomponent Working Fluids for Organic Rankine Cycles (ORCs). *Energy* **1998**, *23*, 449–463. [[CrossRef](#)]
54. Braimakis, K.; Preißinger, M.; Brüggemann, D.; Karellas, S.; Panopoulos, K. Low grade waste heat recovery with subcritical and supercritical Organic Rankine Cycle based on natural refrigerants and their binary mixtures. *Energy* **2015**, *88*, 80–92. [[CrossRef](#)]
55. Chys, M.; van den Broek, M.; Vanslambrouck, B.; de Paepe, M. Potential of zeotropic mixtures as working fluids in organic Rankine cycles. *Energy* **2012**, *44*, 623–632. [[CrossRef](#)]
56. Gu, Z.; Sato, H. Performance of supercritical cycles for geothermal binary design. *Energy Convers. Manag.* **2002**, *43*, 961–971. [[CrossRef](#)]
57. Kanoğlu, M.; Çengel, Y.A. Improving the Performance of an Existing Air-Cooled Binary Geothermal Power Plant: A Case Study. *J. Energy Resour. Technol.* **1999**, *121*, 196–202. [[CrossRef](#)]
58. Kanoğlu, M.; Çengel, Y.A. Retrofitting a Geothermal Power Plant to Optimize Performance: A Case Study. *J. Energy Resour. Technol.* **1999**, *121*, 295–301. [[CrossRef](#)]
59. Karellas, S.; Schuster, A. Supercritical Fluid Parameters in Organic Rankine Cycle Applications. *Int. J. Thermodyn.* **2008**, *11*, 101–108.
60. Schuster, A.; Karellas, S.; Aumann, R. Efficiency optimization potential in supercritical Organic Rankine Cycles. *Energy* **2010**, *35*, 1033–1039. [[CrossRef](#)]

61. Weith, T.; Heberle, F.; Preißinger, M.; Brüggemann, D. Performance of Siloxane Mixtures in a High-Temperature Organic Rankine Cycle Considering the Heat Transfer Characteristics during Evaporation. *Energies* **2014**, *7*, 5548–5565. [[CrossRef](#)]
62. Shu, G.; Wang, X.; Tian, H. Theoretical analysis and comparison of rankine cycle and different organic rankine cycles as waste heat recovery system for a large gaseous fuel internal combustion engine. *Appl. Therm. Eng.* **2016**, *108*, 525–537. [[CrossRef](#)]
63. Quoilin, S.; van den Broek, M.; Declaye, S.; Dewallef, P.; Lemort, V. Techno-economic survey of Organic Rankine Cycle (ORC) systems. *Renew. Sustain. Energy Rev.* **2013**, *22*, 168–186. [[CrossRef](#)]
64. Regulation (EC) No 1005/2009 of the European Parliament and the Council on Substances that Deplete the Ozone Layer; European Union: Brussels, Belgium, 2009.
65. Regulation (EC) No 517/2014 of the European Parliament and of the Council on Fluorinated Greenhouse Gases and Repealing Regulation (EC) No. 842/2006; No European Union: Brussels, Belgium, 2016.
66. Aspen Technology Inc. *Process Optimization for Engineering, Manufacturing and Supply Chain*. V7.3; Aspen Technology Inc.: Burlington, MA, USA, 2011.
67. Sánchez, D.; de Muñoz Escalona, J.; Monje, B.; Chacartegui, R.; Sánchez, T. Preliminary analysis of compound systems based on high temperature fuel cell, gas turbine and Organic Rankine Cycle. *J. Power Sources* **2011**, *196*, 4355–4363. [[CrossRef](#)]
68. Peng, D.-Y.; Robinson, D.B. A New Two-Constant Equation of State. *Ind. Eng. Chem. Fund.* **1976**, *15*, 59–64. [[CrossRef](#)]
69. Boston, J.F.; Mathias, P.M. Phase Equilibria in a Third-Generation Process Simulator. In *Phase Equilibria and Fluid Properties in the Chemical Industry: Proceedings; Part I, Manuscripts of Poster Papers; Part II, Manuscripts of Invited Papers*; Knapp, H., Ed.; Apparatewesen: Frankfurt, Germany, 1980.
70. Müller, A.; Winkelmann, J.; Fischer, J. Backbone family of equations of state: 1. Nonpolar and polar pure fluids. *AIChE J.* **1996**, *42*, 1116–1126.
71. Gross, J.; Sadowski, G. Perturbed-Chain SAFT: An Equation of State Based on a Perturbation Theory for Chain Molecules. *Ind. Eng. Chem. Res.* **2001**, *40*, 1244–1260. [[CrossRef](#)]
72. Angelino, G.; Gaia, M.; Macchi, E. A review of Italian activity in the field of Organic Rankine Cycles. In *ORC-HP-Technology: Working Fluid Problems, Proceedings of the International VDI-Seminar, Zürich, Switzerland, 10–12 September 1984*; VDI-Verlag: Düsseldorf, Germany, 1984; Volume 539, pp. 465–482.
73. Astolfi, M.; Romano, M.C.; Bombarda, P.; Macchi, E. Binary ORC (Organic Rankine Cycles) power plants for the exploitation of medium–low temperature geothermal sources—Part B: Techno-economic optimization. *Energy* **2014**, *66*, 435–446. [[CrossRef](#)]
74. Preißinger, M. *Thermoökonomische Bewertung des Organic Rankine Cycles bei der Stromerzeugung aus Industrieller Abwärme*; Logos Berlin: Berlin, Germany, 2014.
75. Obernberger, I.; Hammerschmid, A.; Bini, A. Biomasse-Kraft-Wärme-Kopplungen auf Basis des ORC-Prozesses - EU Thermie Projekt Admont (A). In *Thermische Nutzung von fester Biomasse: Tagung Salzburg, 16. und 17. Mai 2001*; VDI-Verlag: Düsseldorf, Germany, 2001; Volume 1588, pp. 283–299.
76. Wang, X.-Q.; Li, X.-P.; Li, Y.-R.; Wu, C.-M. Payback period estimation and parameter optimization of subcritical organic Rankine cycle system for waste heat recovery. *Energy* **2015**, *88*, 734–745. [[CrossRef](#)]
77. Quoilin, S.; Declaye, S.; Tchanche, B.F.; Lemort, V. Thermo-economic optimization of waste heat recovery Organic Rankine Cycles. *Appl. Therm. Eng.* **2011**, *31*, 2885–2893. [[CrossRef](#)]
78. Guo, T.; Wang, H.; Zhang, S. Comparative analysis of natural and conventional working fluids for use in transcritical Rankine cycle using low-temperature geothermal source. *Int. J. Energy Res.* **2011**, *35*, 530–544. [[CrossRef](#)]
79. Lee, K.; Kuo, S.; Chien, M.; Shih, Y. Parameters analysis on organic rankine cycle energy recovery system. *Energy Convers. Manag.* **1988**, *28*, 129–136. [[CrossRef](#)]
80. Domingues, A.; Santos, H.; Costa, M. Analysis of vehicle exhaust waste heat recovery potential using a Rankine cycle. *Energy* **2013**, *49*, 71–85. [[CrossRef](#)]
81. Gnielinski, V. Ein neues Berechnungsverfahren für die Wärmeübertragung im Übergangsbereich zwischen laminarer und turbulenter Rohrströmung. *Forsch. Ing.* **1995**, *61*, 240–248. [[CrossRef](#)]
82. Konakov, P. Eine neue Formel für den Reibungskoeffizienten glatter Rohre (Orig. russ.). *Ber. der Akad. der Wissenschaften der UDSSR* **1954**, *51*, 7.
83. Böckh, P.; Wetzels, T. *Wärmeübertragung*; Springer: Berlin/Heidelberg, Germany, 2011.

84. Shah, M.M. A general correlation for heat transfer during film condensation inside pipes. *Int. J. Heat Mass Transf.* **1979**, *22*, 547–556. [[CrossRef](#)]
85. Roetzel, W.; Spang, B. C1 Berechnung von Wärmeübertragern. In *VDI-Wärmeatlas*, 11th ed.; Springer: Berlin/Heidelberg, Germany, 2013; pp. 36–73.
86. Holland, F.; Wilkinson, J. Process Economics: Section 9. In *Perry's Chemical Engineers' Handbook*, 7th ed.; Perry, R.H., Green, D.W., Eds.; McGraw-Hill: New York, NY, USA, 1998.
87. Garrett, D.E. *Chemical Engineering Economics*; Van Nostrand Reinhold: New York, NY, USA, 1989.
88. Andreasen, J.; Kærn, M.; Pierobon, L.; Larsen, U.; Haglind, F. Multi-Objective Optimization of Organic Rankine Cycle Power Plants Using Pure and Mixed Working Fluids. *Energies* **2016**, *9*, 322. [[CrossRef](#)]
89. Baghernejad, A.; Yaghoubi, M. Exergoeconomic analysis and optimization of an Integrated Solar Combined Cycle System (ISCCS) using genetic algorithm. *Energy Convers. Manag.* **2011**, *52*, 2193–2203. [[CrossRef](#)]
90. Shokati, N.; Ranjbar, F.; Yari, M. Comparative and parametric study of double flash and single flash/ORC combined cycles based on exergoeconomic criteria. *Appl. Therm. Eng.* **2015**, *91*, 479–495. [[CrossRef](#)]
91. Van Buijtenen, J. *Kraft aus Wärme durch eine neu Entwickelte ORC Anlage für 80–165 kWe*; VDI-Konferenz “Strom- und Wärmeversorgung in Industrie und Gewerbe”; VDI: Frankfurt, Germany, 2013.
92. Weiß, A.; Zinn, G.; Weith, T.; Preißinger, M.; Brüggemann, D. *Turbinenauslegungsparameter als Kriterium zur Fluidauswahl für ein ORC-Minikraftwerk*; Haus der Technik: Munich, Germany, 2013.
93. Angelino, G.; Invernizzi, C.M.; Macchi, E. Organic working fluid optimization for space power cycles. In *Modern Research Topics in Aerospace Propulsion: In Honor of Corrado Casci*; Angelino, G., Ed.; Springer: New York, NY, USA, 1991; pp. 297–326.
94. Casati, E.; Vitale, S.; Pini, M.; Persico, G.; Colonna, P. Preliminary Design Method for Small Scale Centrifugal ORC Turbines. In *Proceedings of the 2nd International Seminar on ORC Power Systems*, Rotterdam, The Netherlands, 7–8 October 2013.
95. Rinaldi, E.; Buonocore, A.; Pecnik, R.; Colonna, P. Inviscid Stator/Rotor Interaction of a Single Stage High Expansion Ratio ORC Turbine. In *Proceedings of the 2nd International Seminar on ORC Power Systems*, Rotterdam, The Netherlands, 7–8 October 2013.
96. Van Buijtenen, J.; Eppinga, Q.; Ganassin, S. Development and Operation of a High Temperature High Speed Organic Rankine Cycle System. In *Proceedings of the 2nd International Seminar on ORC Power Systems*, Rotterdam, The Netherlands, 7–8 October 2013.
97. Preißinger, M.; Brüggemann, D. Thermal Stability of Hexamethyldisiloxane (MM) for High-Temperature Organic Rankine Cycle (ORC). *Energies* **2016**, *9*, 183. [[CrossRef](#)]
98. *Bundesverband der Energie- und Wasserwirtschaft e.V. BDEW-Strompreisanalyse*; Haushalte und Industrie: Berlin, Germany, 2013.
99. Astolfi, M.; Romano, M.C.; Bombarda, P.; Macchi, E. Thermodynamic ORC Cycle Design Optimization for Medium-Low Temperature Energy Sources. In *Proceedings of the First International Seminar on ORC Power Systems*, Delft, The Netherlands, 22–23 September 2011.
100. Bayerisches Landesamt für Umweltschutz. *Niedertemperaturverstromung Mittels einer ORC-Anlage im Werk Lengfurt der Heidelberger Zement AG*; Auswertung der Messergebnisse aus vier Messkampagnen zur Untersuchung der Anlageneffizienz: Augsburg, Germany, 2001.
101. Sächsische Energieagentur—SAENA GmbH. *Technologien der Abwärmenutzung*; Sächsische Energieagentur SAENA GmbH: Dresden, Germany, 2012.

